CARBON 83 (2015) 217–223

Available at www.sciencedirect.com

ScienceDirect

journal homepage: www.elsevier.com/locate/carbon

Facile synthesis of graphene oxide in a Couette–Taylor flow reactor

Won Kyu Park [a,c,1], Hyeongkeun Kim [a,1], TaeYoung Kim [b], Yena Kim [a,c], Seonmi Yoo [a], Seungdu Kim [a], Dae Ho Yoon [c,*], Woo Seok Yang [a,*]

[a] Electronic Materials and Device Research Center, Korea Electronics Technology Institute, Seongnam 463-816, South Korea
[b] Department of Bionanotechnology, Gachon University, Seongnam 461-701, South Korea
[c] School of Advanced Materials Science and Engineering, Sungkyunkwan University, Suwon 440-746, South Korea

ARTICLE INFO

Article history:
Received 30 June 2014
Accepted 14 November 2014
Available online 20 November 2014

ABSTRACT

A practical approach to bulk-scale graphene-based materials is critically important for their use in the industrial applications. Here, we describe a facile method to prepare graphite oxide (GO) using a Couette–Taylor flow reactor for the oxidation of bulk graphite flakes. We found that the turbulent Couette–Taylor flow in the reactor could be engineered to result in the efficient mixing and mass transfer of graphite and oxidizing agents ($KMnO_4$ and H_2SO_4), thereby improving the efficiency of graphite into GO. As compared to the standard Hummers' method, higher fraction of a single- and few-layer graphene oxide (G-O) can be yielded in a dramatically shortened reaction time, by optimizing the processing parameters, we have shown that ~93% of G-O yield could be achieved within 60 min of reaction time. This method also allowed for the in-situ functionalization of G-O with metal oxide nanoparticles to give a nanoparticle-decorated G-O hybrid material. Our method for facile and large-scale production of graphite oxide may find utility in a range of applications including energy storage, composites and supporting frameworks of catalyst.

1. Introduction

Graphene oxide (G-O) is a two-dimensional material derived from graphene with hydrophilic surface functional groups such as hydroxy, epoxide, and carboxy groups on the basal plane and edges of the graphene. [1,2]. G-O has attracted great attention due to its nature to remain exfoliated in polar solvents as individual layers and be easily reduced back to conductive graphitic materials, referred to as reduced graphene oxide (r-GO) [3–5]. With large surface area and the aforementioned properties, G-O has shown a wide range of applications including electronics, conductive films, energy storage, sensors and composites. [1,6–9].

G-O can be produced in large quantity from bulk graphite by chemical oxidation and subsequent exfoliation [4,10]. While graphite oxide (GO), a stacked galleries of G-O sheets, is synthesized by either the Brodie, Staudenmaier or Hummers method, the most common approach is the use of Hummers method or some variation of this method [3,11,12]. This method involve the oxidation of graphite with strong oxidizing agents such as potassium permanganate ($KMnO_4$) and sulfuric acid (H_2SO_4), which introduces polar oxygen functional groups on the graphene sheet and render it hydrophilic [13–18]. Hence, GO can be readily exfoliated in many polar solvents and disperse particularly well in water, which then can be deposited on substrates to prepare graphitic films by means

* *Corresponding authors:* Fax: +82 31 290 7388 (D.H. Yoon).
E-mail addresses: dhyoon@skku.edu (D.H. Yoon), wsyang@keti.re.kr (W.S. Yang).
[1] These authors equally contributed to this work.
http://dx.doi.org/10.1016/j.carbon.2014.11.024
0008-6223/

of common processing methods such as drop-casting, spraying, or spin-coating [19–22]. In addition, the surface functional groups on GO can serve as sites for functionalization with various active species including metals, oxides, and organic molecules [23,24]. Therefore, the oxidation of graphite into G-O layers provides advantages such as solution processing and derivatization of graphene-based materials for practical use in numerous applications [21,22].

However, oxidation of graphite using the conventional Hummers' method yielded graphite oxide along with a significant amount of non- or under-oxidized graphitic particles under a certain reaction time. To increase yields of graphite oxides that can be exfoliated into single- or few-layer graphene, it often requires either pre-oxidation steps, sequential addition of excess $KMnO_4$, or extended reaction time to several hours [25–27].

To achieve large scale production of individual or few-layer G-O sheets, it is important to oxidize graphite with oxidizing agents penetrating between stacked graphene layers and overcome the strong interlayer van der Waals forces. Efficient oxidation process would give high yields of homogeneously exfoliated G-O sheets in a reduced reaction time.

Herein, we report on a new method to produce a single- or few-layer graphene oxide from bulk graphite with high yields in a significantly shortened reaction time. This method employs Couette–Taylor flow reactor, in which the oxidation of graphite with oxidizing agents (*i.e.* $KMnO_4$, H_2SO_4 and $NaNO_3$) is accelerated by the turbulent Couette–Taylor vortex flow. The Couette–Taylor reactor consists of two coaxial cylinders with the inner one rotating. At a critical rotating speed, toroidal vortices are created and regularly spaced along the cylinder axis [28–30]. We found that this toroidal motion of fluids leads to highly efficient radial mixing of graphite and oxidizing agents in the system, thereby enhancing the oxidation efficiency. As compared to the conventional Hummers method, the use of this system allows for the production of a single or few-layer G-O at a high yield within an hour of reaction time. In this work, a series of oxidation reaction was carried out in a Couette–Taylor reactor with respect to processing parameters such as rotating speeds and reaction time, and the results will be discussed in terms of yield of G-O. This method is also compatible with the continuous production of G-O sheets and the functionalization of G-O with other species such as metal oxides can be achieved simultaneously.

2. Experimental details

2.1. Synthesis of G-O

Graphite flakes were oxidized using Couette–Taylor flow reactor. 5 g of graphite flakes (SP-1 graphite, 50 μm) and 3.75 g of sodium nitrate ($NaNO_3$) were added to 169 mL of sulfuric acid (H_2SO_4, 95%). Then, 23 g of potassium permanganate ($KMnO_4$) was slowly added to this mixture at 10 °C or lower and the mixture was stirred for 30 min. The Couette–Taylor flow reactor (length: 400 mm) consists of two coaxial cylinders with the fixed outer cylinder (radius: 125 mm) and the rotating inner cylinder (radius: 25 mm). After the mixture was introduced into the gap between the two cylinders, the inner cylinder was rotated. The rotating speed of the inner cylinder was varied from 400 to 1200 rpm for the reaction time of 15, 30, 45 and 60 min. Oxidation of graphite in a Couette–Taylor flow reactor led to a brown-colored pasty slurry within 60 min. For a work-up, 200 mL of purified water and 10 mL of peroxide (H_2O_2, 30%) were added to the mixture, and then stirred for 60 min. For purification, a filter press system was used to separate GO and impurities. As detailed in Supporting Information, the filter press system consists of a membrane filter plates with a pore size of 5 μm. GO slurry and a large volume of DI water was continually fed into the system until the water and impurities is squeezed out. The purification step was done for 6 h. The remaining GO solids were collected, dispersed and sonicated in water. Then, non- or under-oxidized graphitic particles were precipitated out by further centrifugation at 4000 rpm for 30 min. The supernatant containing single- or few-layer G-O was filtered over a PTFE membrane with a 1 μm pore size and vacuum- or freeze-dried for characterization.

2.2. Characterization

The microstructure of the samples was investigated using a field emission scanning electron microscopy (FESEM, JSM-7600F, JEOL), and a high resolution transition electron microscopy (HRTEM, JEM-3010, JEOL). The thickness of the G-O sheets were obtained using atomic force microscopy (AFM, SPA-300HV, SII). X-ray diffraction (XRD) patterns of oxidized graphite prepared were determined by a D8 ADVANCE (Bruker Corporation) with Cu-Kα X-ray source. Raman spectra were obtained by micro-Raman system (Bruker FRA 160/S, Burker) with an excitation energy of 2.41 eV (514 nm). X-ray photoelectron spectroscopy (XPS) spectrum of the G-O sample were performed by a VG Microtech ESCA2000 (JEOL) with a monochromatic Al-Kα X-ray source at 250 W.

3. Results and discussion

According to the modified Hummers method, graphite oxide is produced by the oxidation of bulk graphite in the acidic oxidizing medium [4,10]. In the course of the reaction, the oxidation begins by the oxidizing agent attacking graphene layer. To afford the efficient oxidation of graphite, it would be important to enhance the rate of diffusion of the oxidizing agent into the graphite interlayer and the subsequent oxidation reaction. To this end, we used a Couette–Taylor flow reactor for the efficient mixing and mass transfer of graphite and oxidizing agents, thereby enhancing an efficiency of oxidation reaction of graphite into graphite oxide.

Fig. 1 illustrates the reaction system used for the oxidation of bulk graphite with oxidizing agent. As shown in Fig. 1a, the Couette–Taylor reactor consists of two concentric cylinders and the inner cylinder rotates at a controlled speed while the outer cylinder is kept stationary [28–30]. Then, a mixture of graphite flakes, the concentrated acids and oxidizing agents were fed into the reactor. As the rotation speed of the inner cylinder reaches a critical value, it develops the counter-rotating toroidal vortices in a regular arrangement

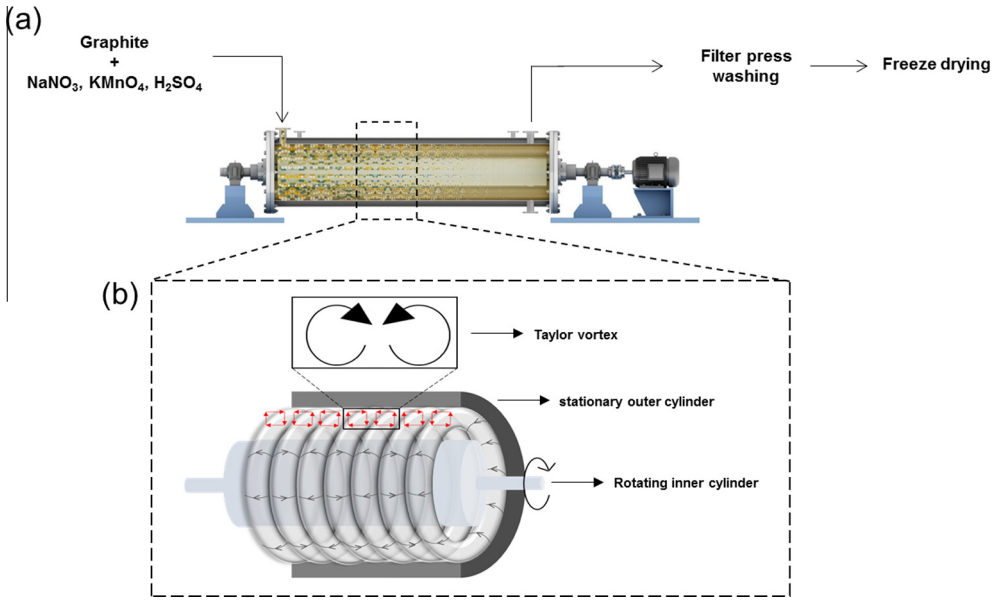

Fig. 1 – Illustration of the oxidation reaction of graphite flakes in the Couette–Taylor flow reactor. (a) Schematic diagram of Couette–Taylor flow reactor system. (b) Conceptual diagram of Vortex structure in the Couette–Taylor reactor. (A color version of this figure can be viewed online.)

along the cylinder axis (Fig. 1b). This Couette–Taylor vortex induces highly effective radial mixing within each vortex cell and uniform fluidic motion enabling enhanced mass transfer of the reactants. This toroidal motion also causes a high wall shear stress that is expected to improve the dispersion of graphite in an acidic oxidizing medium and the rate of diffusion of the oxidizing agent into the graphite interlayer.

In the Couette–Taylor reactor, the hydrodynamic condition of the fluids is dependent on the rotating speed of the inner cylinder. The Couette–Taylor vortex can be formed when the Taylor number proportional to the angular velocity of the inner cylinder exceeds a critical value [28–30]. In this sense, we first carried out the oxidation of graphite in the reactor with increasing rotating speeds from 400 to 1200 rpm for the reaction time of 60 min. Fig. 2 shows the X-ray diffraction (XRD) patterns for the product synthesized with respect to the rotating speed. When the rotation speed of inner cylinder was 400 rpm or less, a diffraction peak was observed at 26.5° 2θ angle with the interlayer spacing of 0.34 nm, indicating the dominance of non-oxidized graphite. As the rotation speed exceeds 400 rpm, the peak associated with the non-oxidized graphite is no longer present and new peaks were found at ~10.5° corresponding to the interlayer spacing of ~0.9 nm. This indicates that the rotation speed larger than 400 rpm is required for the formation of Couette–Taylor vortex that can lead to the efficient oxidation reaction of graphite. Based on this result, the rotation speed of 600 rpm was used for the following set of experiments.

In the following experiment, we varied the reaction time from 15 to 60 min, while a rotating speed of inner cylinder was set as 600 rpm. Fig. 3 shows the field emission scanning electron microscopy (FESEM) image of the oxidized graphite treated in a Couette–Taylor flow reactor for different reaction time (15, 30, 45 and 60 min). The graphite oxide flakes sampled through freeze-drying from the reaction mixture have

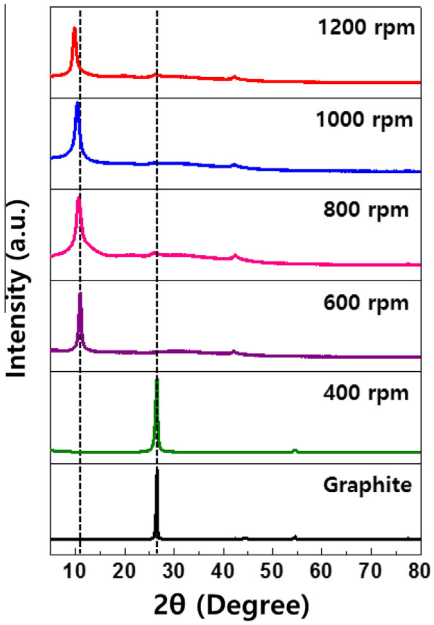

Fig. 2 – XRD patterns for the oxidized graphite synthesized in a Couette–Taylor flow reactor with respect to rotating speed of inner cylinder (400, 600, 800, 1000 and 1200 rpm). (A color version of this figure can be viewed online.)

different morphologies with respect to the reaction time. A sample taken at the reaction time of 15 min showed mostly thick layered platelets and graphitic particles. This is likely due to the insufficient reaction time for the acids and oxidizing agent to penetrate the gaps between the carbon layers of the graphite powder, resulting in partially oxidized graphite. As the reaction time is extended, the graphite flakes were expanded in the form of highly oxidized graphite and showed

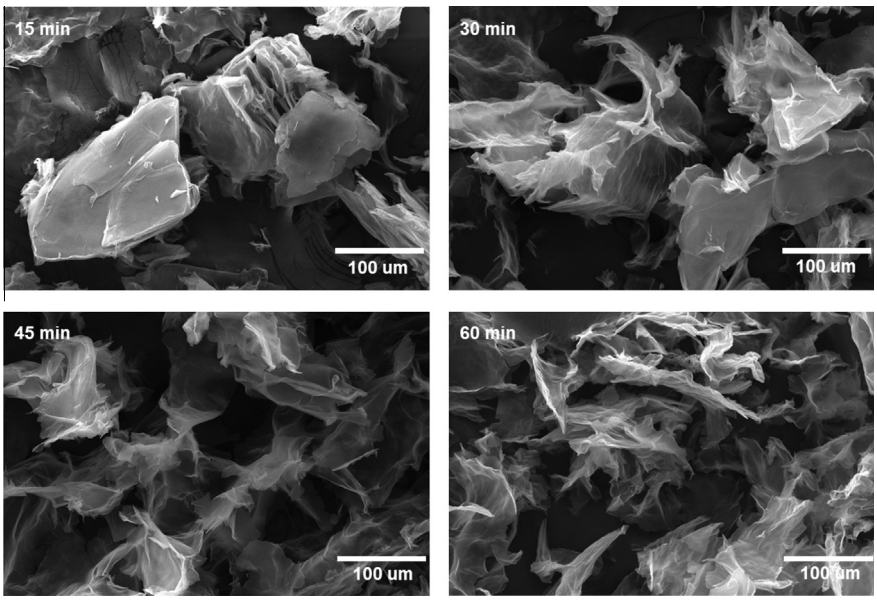

Fig. 3 – FE-SEM images of the oxidized graphite synthesized in the Couette–Taylor flow reactor with respect to the reaction time (15, 30, 45 and 60 min) (scale bar: 100 μm).

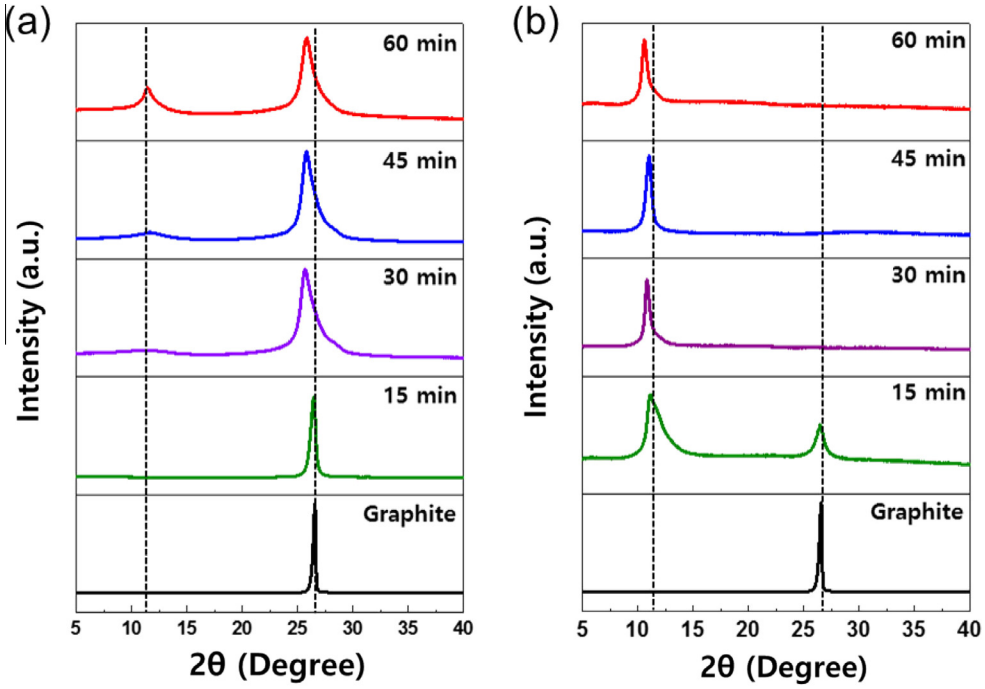

Fig. 4 – XRD patterns of the graphite oxide powders prepared according to (a) Hummers method and (b) the method using the Couette–Taylor flow reactor, depending on the reaction time (15, 30, 45 and 60 min). (A color version of this figure can be viewed online.)

thin crumpled sheet morphologies. These results suggest that the reaction time of 60 min is sufficient to yield highly oxidized form of graphite.

To compare the efficiency of the Couette–Taylor flow method and the Hummers' method, the progression of oxidation reaction with respect to the reaction time was examined. For both cases, the concentration of graphite flake and oxidizing agents was kept the same. Fig. 4 shows XRD patterns of oxidized graphite prepared using the Couette–Taylor reactor and the Hummers method. The interlayer spacing was 0.34 nm ($2\theta = 26.4°$) for the starting graphite flake and increased to ~0.78 nm ($2\theta = 10.3°$) for the oxidized graphite sample. Even for the reaction time of 60 min, the sample prepared by the Hummers' method showed two XRD peaks,

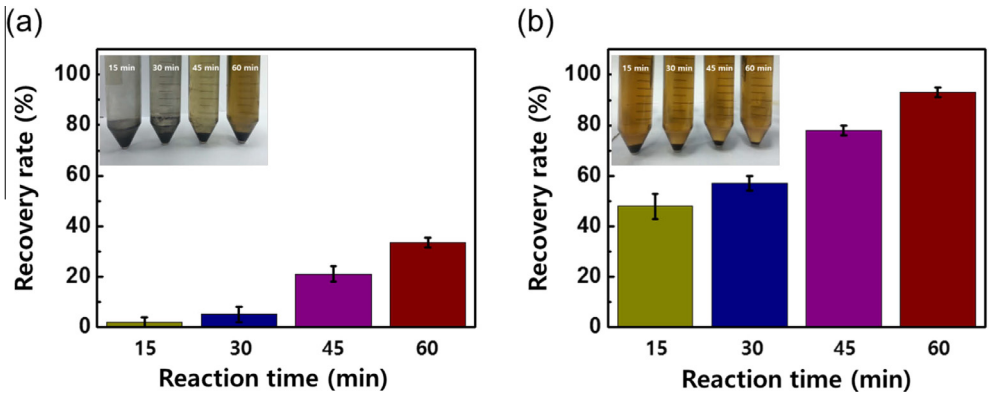

Fig. 5 – Recovery rate of the graphene oxide obtained with respect to the reaction time for (a) the Hummers' method and (b) the Couette–Taylor flow reactor. (Inset) Photograph of the samples after the dispersion in water, sonication and centrifugation. Precipitates represents non- or under-oxidized graphite flakes. (A color version of this figure can be viewed online.)

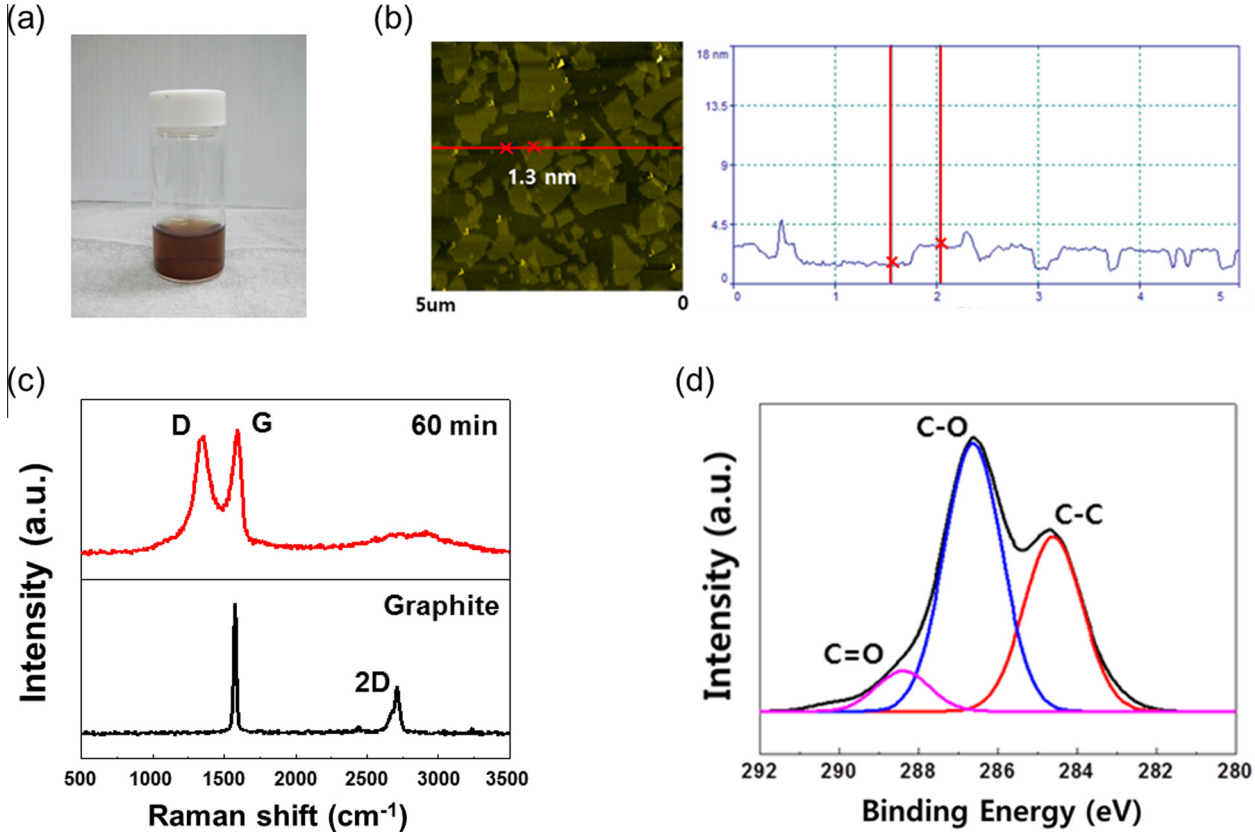

Fig. 6 – Characterization of the G-O prepared using the Couette–Taylor flow reactor (reaction time: 60 min). (a) Photograph of the aqueous suspension (1 mg/mL) of G-O. (b) Tapping-mode AFM image and height profile of the G-O sheets. The measured thickness of the G-O sheet layer was 1.3 nm. (c) Raman spectra of the graphite flake and G-O (514 nm laser excitation). (d) C1s XPS spectra of the G-O. (A color version of this figure can be viewed online.)

indicating that the significant amount of the non-oxidized graphite flakes were still retained in the sample. In a sharp contrast, the sample prepared using the Couette–Taylor flow reactor no longer showed the characteristic peak of graphite after 30 min of reaction time and exhibited a diffraction pattern typical for highly oxidized graphite oxide. Therefore, this result indicates that the oxidation of graphite flakes into graphite oxide can be achieved in a significantly shortened reaction time by using the Couette–Taylor flow reactor.

As compared to the conventional Hummers' method, the increased efficiency of this method was apparent after isolation of non- or under-oxidized graphitic particles. The

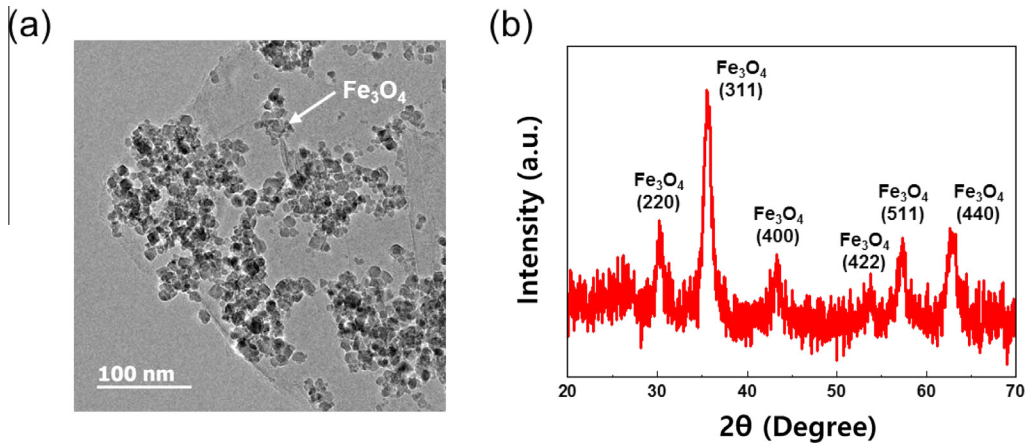

Fig. 7 – The Fe_3O_4@GO prepared using the Couette–Taylor flow reactor. (a) TEM image and (b) XRD pattern of Fe_3O_4@GO. (A color version of this figure can be viewed online.)

oxidation reaction of graphite was carried out for different times and the resulting carbon solids were exfoliated in water, followed by centrifugation. During centrifugation, non- or under-oxidized graphitic particles were precipitated out, while highly oxidized graphite is retained in the supernatant. Note that the highly oxidized graphite in the supernatant corresponds to the single- or few-layer graphene oxide and its measured weight relative to that of the initial carbon solids was used to give the recovery rate. Fig. 5 compares the recovery rates of the G-O prepared by the Hummers and the Couette–Taylor flow method. In case of the Hummer method, the recovery rate was ~37% for the reaction time of 60 min, indicating than more than 60% of under-oxidized graphite particles were present in the products. For the Couette–Taylor flow method, the recovery rate was increased to ~93% indicating most of the graphite flakes were oxidized and exfoliated into single- or few-layered graphene oxide. This result supports that the use of Couette–Taylor flow reactor can afford the efficient oxidation of graphite into highly oxidized graphite oxide in a significantly shortened reaction time.

For characterization, the oxidized graphite obtained by 60 min reaction in the Couette–Taylor flow reactor were collected, followed by the subsequent purification and isolation. The oxidized graphite was then exfoliated in water with mild sonication, forming a colloidal suspension of G-O. Atomic force microscopy (AFM) images and the height profile (Fig. 6b) of G-O sheets revealed the presence of sheets with uniform thickness (~1.3 nm), typical of the highly oxidized individual G-O sheet. Raman spectrum of G-O (Fig. 6c) showed G peak at ~1590 cm^{-1} and D peak at ~1350 cm^{-1}. In the Raman spectrum of G-O, the G band was broadened as compared to that of graphite flake, and D-band became prominent, confirming the presence of oxidized graphitic domains. Fig. 6d shows the C1s X-ray photoelectron spectroscopy (XPS) spectrum of the G-O sample with three components corresponding to carbon atoms with the oxygen functional group. In the spectrum, the deconvoluted peaks at 284.5, 286.7, and 288.2 eV correspond to the sp^2 carbon in aromatic ring, the epoxy/hydroxyls (C—O), and the carbonyl (C=O), respectively. The percentage of the oxidized carbon indicates a degree of oxidation corresponding to the highly oxidized graphite oxide.

Based on these results, the oxidation reaction of graphite flakes in the Couette–Taylor flow reactor enables the facile production of highly oxidized single- or few-layer G-O on large-scale.

Along with the facile and large-scale production, our method using the Couette–Taylor flow reactor has advantages over Hummers' method in that it is compatible with the continuous production of G-O sheets. Furthermore, the functionalization of G-O sheets can also be achieved in a way that G-O and metal oxide nanoparticles are synthesized in the same reactor to produce nanoparticle-decorated G-O sheets. For this experiment, metal salt aqueous solution was introduced into the reactor in the course of oxidation reaction of graphite flakes. Subsequently, the metal oxide nanoparticle nucleated and grew on the G-O surfaces to result in G-O sheets decorated with 10 nm-sized Fe_3O_4 nanoparticles, as shown in Fig. 7.

4. Conclusions

In summary, we have demonstrated a method to accelerate the oxidation process of bulk graphite into graphite oxide with high yields. We found that the use of Couette–Taylor flow reactor leads to the efficient mixing and mass transfer of graphite and oxidizing agents, thereby enhancing the oxidation efficiency. By adaptation of this method, high fraction of a single or few-layer graphene oxide was produced in a significantly shortened reaction time. From the perspective of large-scale production of G-O, this method has advantages over the conventional Hummers' method as it is compatible with the continuous production. Moreover, the method allows for the in-situ functionalization of G-O with metal oxide nanoparticles and afforded a nanoparticle-decorated G-O hybrid material. Our method for facile and large-scale production of highly oxidized graphite may find utility in various applications, including energy storage, composites and supporting frameworks of catalyst.

Author contributor

W.S.Y. and D.H.Y. planned and supervised the project; H.K assisted in supervision; T.Y.K. advised the project; W.K.P., H.K. conceived and did the experiment and analyzed the properties of G-O and Fe_3O_4@GO; W.S.Y., D.H.Y., H.K. and W.K.P. analyzed data and wrote the manuscript; Y.K., S.Y. and S.K. helped with the synthesis of G-O and measurement of its characteristics.

Acknowledgements

This work was supported by Energy Efficiency & Resources of the Korea Institute of Energy Technology Evaluation and Planning (KETEP) grant funded by the Korea government Ministry of Knowledge Economy (No. 20142010102690), Energy Efficency & Resources of the Korea Insitute of Energy Technology Evaluation and Planning (KETEP) grant funded by the Korea government Ministry of Knowledge Economy (No. 2012T100201723). This work also was supported by Basic Science Research Program through the National Research Foundation of Korea (NRF) funded by the Ministry of Education, Science and Technology (NRF-2013R1A2A2A01010027).

Appendix A. Supplementary data

Supplementary data associated with this article can be found, in the online version, at http://dx.doi.org/10.1016/j.carbon.2014.11.024.

REFERENCES

[1] StankovichS DikinDA, Dommett GHB, Kohlhaas KM, Zimney EJ, Ruoff RS, et al. Graphene-based composite materials. Nature 2006;442:282–6.
[2] Dreyer DR, Park S, Bielawski CW, Ruoff RS. The chemistry of graphene oxide. Chem Soc Rev 2010;39:228–40.
[3] Hummers WS, Offeman RE. Preparation of graphitic oxide. J Am Chem Soc 1958;80:1339.
[4] Stankovich S, Dikin DA, Piner RD, Kohlhaas KA, Kleinhammes A, Ruoff RS. Synthesis of graphene-based nanosheets via chemical reduction of exfoliated graphite oxide. Carbon 2007;45:1558–65.
[5] Stankovich S, Piner RD, Chen X, Wu N, Nquyen ST, Ruoff RS. Stable aqueous dispersions of graphitic nanoplatelets via the reduction of exfoliated graphite oxide in the presence of poly(sodium 4-styrenesulfonate). J Mater Chem 2006;16:155–8.
[6] Wang Y, Shi Z, Huang Y, Ma Y, Wang C, Chen M, et al. Supercapacitor devices based on graphene materials. J Phys Chem C 2009;113:13103–7.
[7] Schedin F, Geim AK, Morozov SV, Hill EW, Blake P, Novoselov KS, et al. Detection of individual gas molecules adsorbed on graphene. Nat Mater 2007;6:652–5.
[8] Zhou M, Zhai Y, Dong S. Electrochemical sensing and biosensing platform based on chemically reduced graphene oxide. Anal Chem 2009;81:5603–13.
[9] Watcharotone S, Dikin DA, Stankovich S, Piner R, Jung I, Liu CP, et al. Graphene–silica composite thin films as transparent conductors. Nano Lett. 2007;7:1888–92.
[10] Park S, Ruoff RS. Chemical methods for the production of graphenes. Nat Nanotechnol 2009;4:217–24.
[11] Brodie BC. Sur le poids atomique du graphite. Ann Chim Phys 1860;59:466.
[12] Staudenmaier L. Verfahren zur Darstellung der Graphitsäure. Ber Deut Chem Ges 1898;31:1481–7.
[13] Kotov NA, Dekany I, Fendler JH. Ultrathin graphite oxide–polyelectrolyte composites prepared by self-assembly: transition between conductive and non-conductive states. Adv Mater 1996;8:637–41.
[14] Cassagneau T, Guerin F, Fendler JH. Preparation and characterization of ultrathin films layer-by-layer self-assembled from graphite oxide nanoplatelets and polymers. Langmuir 2000;16:7318–24.
[15] Kovtyukhova NI et al. Layer-by-layer assembly of ultrathin composite films from micron-sized graphite oxide sheets and polycations. Chem Mater 1999;11:771–8.
[16] Hirata M, Gotou T, Ohba M. Thin-film particles of graphite oxide 2: preliminary studies for internal micro fabrication of single particle and carbonaceous electronic circuits. Carbon 2005;43:503–10.
[17] Szabo T, Szeri A, Dekany I. Composite graphitic nanolayers prepared by self-assembly between finely dispersed graphite oxide and a cationic polymer. Carbon 2005;43:87–94.
[18] Dimiev AM, Tour JM. Mechanism of graphene oxide formation. ACS Nano 2014;8:3060–8.
[19] Titelman GI, Gelman V, Bron S, Khalfin RL, Cohen Y, Bianco-Peled H. Characteristics and microstructure of aqueous colloidal dispersions of graphite oxide. Carbon 2005;43:641–9.
[20] Szabo T, Tombacz E, Illes E, Dekany I. Enhanced acidity and pH-dependent surface charge characterization of successively oxidized graphite oxides. Carbon 2006;44:537–45.
[21] Li D, Muller MB, Gilje S, Kaner RB, Wallace GG. Processable aqueous dispersions of graphene nanosheets. Nat Nanotechnol 2008;3:101–5.
[22] Becerril HA, Mao J, Liu Z, Stoltenberg RM, Bao Z, Chen Y. Evaluation of solution-processed reduced graphene oxide films as transparent conductors. ACS Nano 2008;2:463–70.
[23] Ramanathan T, Abdala AA, Stankovich S, Dikin DA, Alonso MH, Ruoff RS, et al. Functionalized graphene sheets for polymer nanocomposites. Nat Nanotechnol 2008;3:327–31.
[24] Scheuermann GM, Rumi L, Steurer P, Bannwarth W, Malhaupt R. Palladium nanoparticles on graphite oxide and its functionalized graphene derivatives as highly active catalysts for the Suzuki–Miyaura coupling reaction. J Am Chem Soc 2009;131:8262–70.
[25] Marcano DC, Kosynkin DV, Berlin JM, Sinitskii A, Sun Z, Tour JM, et al. Improved synthesis of graphene oxide. ACS Nano 2010;4:4806–14.
[26] Bao C, Song L, Xing W, Yuan B, Wilkie CA, Hu Y, et al. Preparation of graphene by pressurized oxidation and multiplex reduction and its polymer nanocomposites by masterbatch-based melt blending. J Mater Chem 2012;22:6088–96.
[27] Chandra V, Park J, Chun Y, Lee JW, Hwang IC, Kim KS. Water-dispersible magnetite-reduced graphene oxide composites for arsenic removal. ACS Nano 2010;4:3979–86.
[28] Taylor GI. Stability of a viscous liquid contained between two rotating cylinders. Phil Trans R Soc Lond Ser A 1923;223:289–343.
[29] Brandstater A, Swift J, Swinney HL, Wolf A, Farmer JD, Crutchfield JP, et al. Low-dimensional chaos in a hydrodynamic system. Phys Rev Lett 1983;51:1442.
[30] Gu ZH, Fahidy TZ. Visualization of flow patterns in axial flow between horizontal coaxial rotating cylinders. Canad J Chem Eng 1985;63:14–21.